



## A powerful tracking detector for cosmic rays: the magnetic spectrometer of the PAMELA satellite experiment

O. Adriani<sup>a</sup>, L. Bonechi<sup>a\*</sup>, M. Bongi<sup>a</sup>, G. Castellini<sup>b</sup>, R. D'Alessandro<sup>a</sup>, A. Gabbanini<sup>b</sup>, M. Grandi<sup>a</sup>, P. Papini<sup>a</sup>, S. B. Ricciarini<sup>a</sup>, P. Spillantini<sup>a</sup>, S. Straulino<sup>a</sup>, F. Taccetti<sup>a</sup>, M. Tesi<sup>b</sup>, E. Vannuccini<sup>a</sup>

<sup>a</sup>Università degli Studi di Firenze and INFN Sezione di Firenze, Firenze, Italy

<sup>b</sup>Istituto di Fisica Applicata "Nello Carrara", CNR, Firenze, Italy

The WiZard-PAMELA detector will be ready within some months to be installed on board of the Russian satellite Resurs-DK1. The satellite will follow, for at least 3 years, a quasi polar orbit with an inclination of 70.4° with respect to the equatorial plane. The experiment will allow the measurement of the antiproton and positron spectra within a wide momentum range and the search for light anti-nuclei in cosmic rays. The detector subsystems have been tested and the final assembly phase is in progress. In this paper we describe the structure of the PAMELA magnetic spectrometer, its current status and some precautions taken to satisfy the requirements of the mission.

### 1. Introduction

PAMELA (Payload for Antimatter Matter Exploration and Light-nuclei Astrophysics [1–3]) is a satellite-borne experiment developed by the WiZard collaboration and dedicated to cosmic ray measurements.

The goals of the experiment are mainly the measurements of the antiproton and positron spectra in cosmic rays outside the atmosphere, in an very large energy range. Existing data, obtained by several previous experiment [3–5], cover a momentum range between about 100 MeV/c and 50 GeV/c. All these data are in agreement with the theoretical predictions based upon a secondary production of antiproton and positron in primary cosmic rays interactions with interstellar medium (ISM). It is important, nevertheless, to remark that data for momenta above a few GeV/c have great uncertainties due, essentially, to low statistics<sup>2</sup>. It is thus impossible to use these data to distinguish among different predictions and, for example, to put in evidence a possible antiparticles flux contribution given

by Dark Matter (DM) annihilation in the galactic halo. PAMELA will allow precise measurements of antiproton spectrum between 80 MeV/c and 190 GeV/c and of positron spectrum between 50 MeV/c and 270 GeV/c with high statistics. This will allow us to test the models for antiparticles production and propagation and to determine a possible DM signature. Moreover the spectra of light nuclei will be studied and the search for light antinuclei will be carried on with high sensitivity (of the order of 10<sup>-7</sup> in the  $\bar{\text{H}}/\text{H}$  ratio). The existence of antinuclei in CR would indicate the existence of antimatter galaxies where these particles could be produced.

The accurate particle discrimination and precise momentum measurement capabilities of PAMELA, coupled to the long (3 years) data taking period, make these goals attainable. The payload is composed of several subdetectors (figure 1): a scintillator Time Of Flight (used also for the *trigger* signal), a Transition Radiation Detector, a magnetic spectrometer, an imaging calorimeter, an anticoincidence system and an additional scintillator at the end. The magnetic spectrometer, described in this paper, is the core of the apparatus, and it is used for the measurement of particles momenta and charge sign.

\*Corresponding author.

Email address: lorenzo.bonechi@fi.infn.it

<sup>2</sup>All these experiment but AMS were balloon-borne experiment and so they had short time length and a high background due to residual atmosphere.

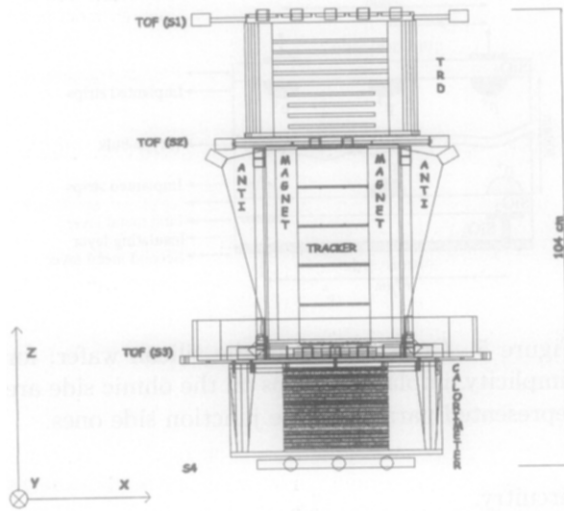


Figure 1. Detector scheme.

## 2. The magnetic spectrometer

The spectrometer consists of a magnetic system and a tracking system that have been developed, assembled and tested by the WiZard-Firenze INFN group. A great effort in the development of this detector has been made to satisfy all the requirements of the mission, imposed by the satellite specifications and by the physics goals.

### 2.1. Magnetic system

The magnetic system is divided into five modules of *Vacodym 335 HR* (a Nd–Fe–B alloy with a residual magnetization of about 1.3 T) assembled in such a way as to form a cavity of  $131 \times 161 \text{ mm}^2$  surface and 445 mm height. Each of these blocks is composed of 16 magnetized pieces with triangular section that are glued together to give the configuration shown in figure 2.

This configuration has been chosen to have very high and uniform field strength and uniformity inside the cavity and the lowest possible field intensity outside. To protect the magnetic material from chemical attacks and slow down its aging, a  $500 \mu\text{m}$  aluminum layer covers all the free surfaces of the magnet. The magnetic field has been mapped by means of an FW-Bell 9950 gaussmeter equipped with a three-axis Hall probe mounted

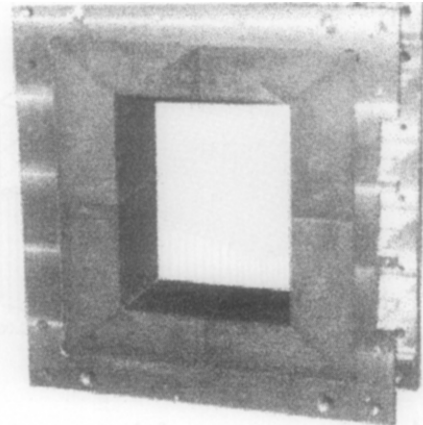
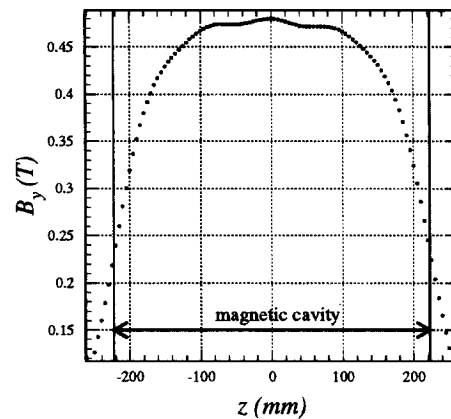


Figure 2. A prototype magnetic block.

on an automatic positioning device. In figure 3 the measured main field component ( $B_y$ ) is plotted as a function of the  $z$  coordinate (see fig. 1) for the central axis of the cavity. As showed in the graph, its value reaches 0.48 T in the center of the cavity ( $z=0$ ) and remains nearly constant in a wide region. The good uniformity of the field is evident also in figure 4, where  $B_y$  is plotted for the central section of the magnetic cavity ( $xy$  plane).

Figure 3. Main component of the magnetic field plotted as a function of the  $z$  coordinate along the central axis coordinate of the cavity (see fig 1).

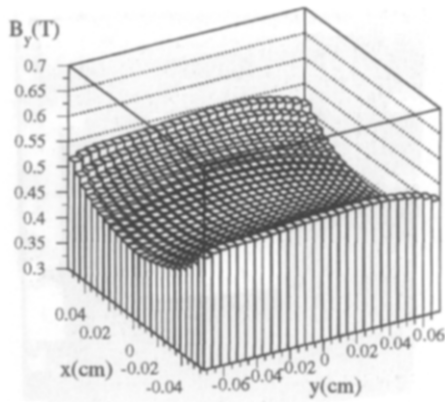


Figure 4. Main component of the magnetic field plotted for the central section ( $xy$  plane,  $z=0$  mm) of the magnetic cavity.

**2.2. Tracking system**

The tracking system [6] consists of six detector planes based upon high precision double-sided microstrip silicon sensors [7]. The sensors are high resistivity n-type silicon cut in  $(53.33 \times 70.00)$  mm<sup>2</sup> wafers, 300  $\mu$ m thick (figure 5). 2035 p<sup>+</sup> type microstrips are implanted on the junction side with an implantation pitch of 25  $\mu$ m. On the ohmic side there are 1024 n<sup>+</sup> type microstrips (alternated to p<sup>+</sup> blocking strips) with implantation pitch of 67  $\mu$ m. These are disposed orthogonally to the junction side ones. Decoupling capacitors are directly integrated on the sensors by mean of a silicon dioxide deposition, 100 nm thick, placed between the implanted strips and the metal readout strips. On the ohmic side a second metal layer is present to carry the microstrip signals to the front-end electronics. The readout pitch is 50  $\mu$ m on both sides.

The detector plane, main structure of the tracking system, is assembled from three basic detection units, called *ladders* (figure 6). The *ladder* consists of two silicon sensors and one *hybrid* circuit. The *hybrid* is a double sided alumina which houses the front-end electronics. Its geometrical dimensions are  $(53.33 \times 50.00)$  mm<sup>2</sup> and its thickness 300  $\mu$ m. Each side is equipped with eight VA1 chips. The VA1 consists of 128 charge sensitive preamplifiers, each connected to a CR-RC shaper and followed by a sample and hold

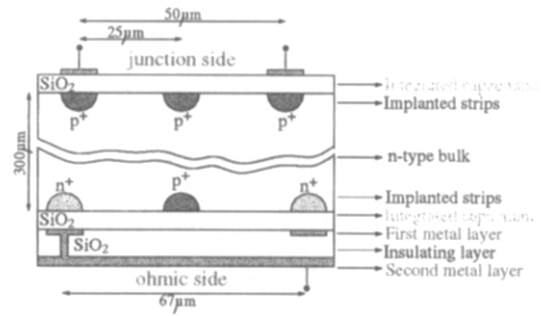


Figure 5. Cross section of the silicon wafer; for simplicity, implanted strips on the ohmic side are represented parallel to the junction side ones.

circuitry.

The hybrid and sensors of a *ladder* are glued head to head using Araldite AY 103 with HY 951 hardener. The plane structure, figure 7, is obtained by placing three *ladders* side by side and gluing them not directly, but to four rigid carbon fiber bars (horizontal black lines in the figure). The material used for these stiffeners has a high Young modulus (200 GPa) and gives the neces-

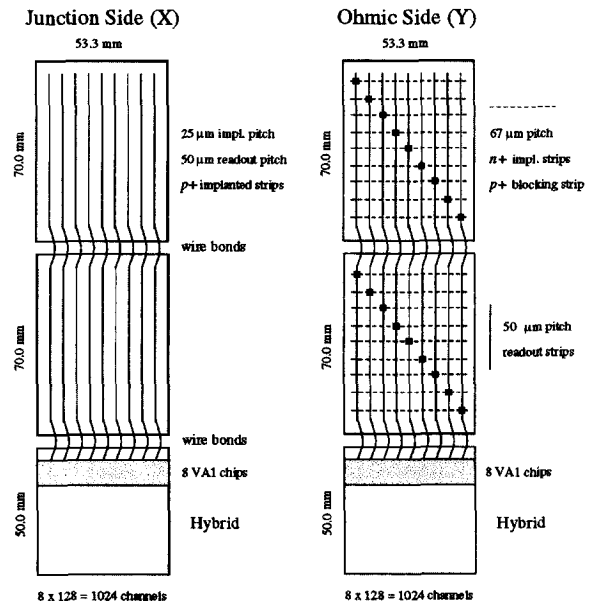


Figure 6. The *ladder* structure: tracking system basic detection unit.

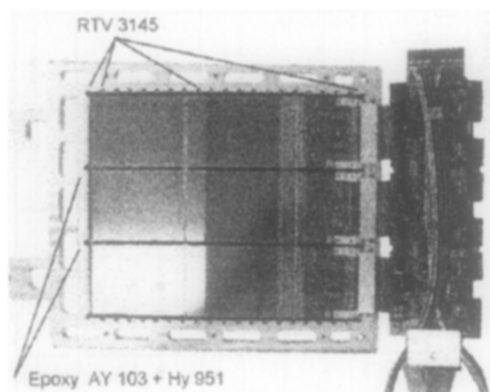


Figure 7. One of the six flight model planes inserted in the aluminum frame. From left to right: silicon sensors, *hybrid* circuits, read-out boards.

sary rigidity to the plane. It is the first time that such a structure will be used on a space mission and it was chosen so as to avoid introducing further material, which causes multiple scattering, under or above the silicon sensors. In this way we reduce the spillover background and improve the momentum resolution at low energy.

The three *hybrids* are connected to the read-out electronics by means of each 38 pins kapton cables 50 mm long. Each plane is fixed in an aluminum frame, by mean of 46 gluing points along the carbon fibre bars, as showed in figure 7. Two of these points are rigid (Araldite AY 103 with HY 951 hardener) while all the others are elastic (Silicone Dow Corning RTV 3145). This is the best compromise that has been found between a rigid configuration (that guarantees the survival of the structure during the launch phase) and an elastic one (that gives the best resistance to thermal fatigue).

Four detector planes are placed in between adjacent magnetic blocks and the other two sit at the entrances of the magnetic cavity. The distance between the planes in this configuration is 89 mm. The electronics boards are lodged on the magnetic tower to achieve the compact structure showed in figure 8. A thin ( $2.5\mu\text{m}$ ) mylar film has been applied on the aluminum frames in order to have a mechanical protection layer between each pair of planes.

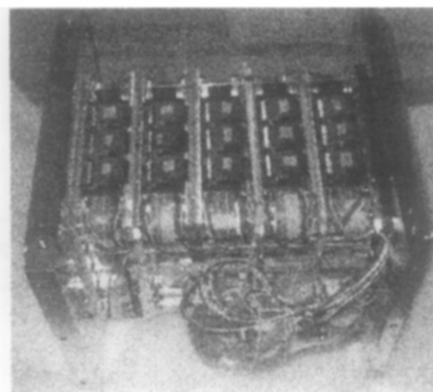


Figure 8. The flight model magnetic spectrometer, assembled in June 2002.

### 2.3. Beam tests at CERN

Several beam tests have been done since 1996 to investigate the tracking performances. Tests were made using a smaller telescope composed of five single *ladders* and a permanent magnet with a cavity ( $56 \times 56 \times 210$ ) mm<sup>3</sup>. The results (showed in fig. 9 for a *ladder*) confirm the good spatial resolution: about  $3\mu\text{m}$  on the junction side (bending view) and  $11.5\mu\text{m}$  on the ohmic side, achieved by means of S/N ratios of about 50 and 25 respectively [8].

### 3. Thermal test

The PAMELA detector is equipped with a isooctane cooling loop; the fluid temperature runs between  $5^\circ\text{C}$  and  $35^\circ\text{C}$ . The magnetic tower mechanics is in thermal contact with the cooling loop and represents the sink for the heat generated by the frontend electronics. Due to the structure of the plane and the absence of gravity, the main contribution to the heat exchange is given by the radiative losses. These losses mainly depend on the absorption coefficient of the inner surfaces of the magnet. Starting from 2002, tests were performed to measure the temperature of VA1 *chips* for different treatment of the surfaces<sup>3</sup>. A detector plane was inserted between two adjoining dummy magnetic blocks placed in

<sup>3</sup>Standard spray black and silver paints and Nextel Velvet Coating 811-21 (with Verdunner 8061) were used.

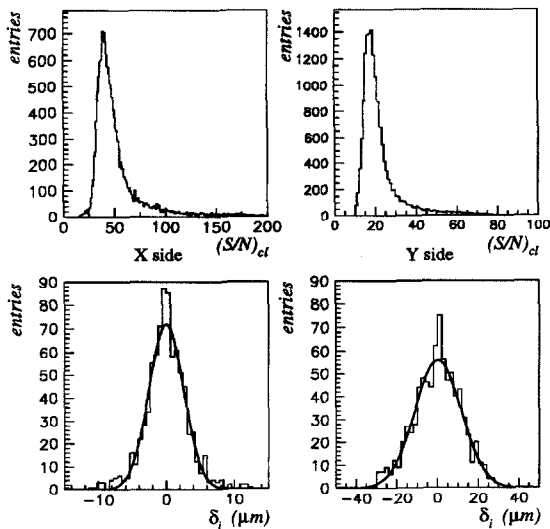


Figure 9. S/N ratio and positional residual distributions for the two sides of a *ladder*. The resolutions obtained for this *ladder* are  $\sigma_x=(2.86\pm 0.10)\mu\text{m}$  and  $\sigma_y=(12.3\pm 0.4)\mu\text{m}$ . The mean values for the S/N ratio are  $(S/N)_x = 52.3$  and  $(S/N)_y = 22.7$  [8].

a vacuum chamber to avoid air convection. Two PT1000 resistors were used to measure the temperatures of a VA1 of the middle *ladder* and of the iron block. In figure 10 the temperature difference  $\Delta T$  between the two sensors is plotted as a function of time interval starting from the time the electronics were switched on. It is clear that the Nextel paint coating gives a better radiative energy transfer between the VA1s and the metal blocks around: the  $\Delta T$  equilibrium value results about  $6.5^\circ$  lower with respect to the bare iron case. For this reason, the cavity walls and the surfaces between each couple of magnetic blocks (especially the regions near the VA1s) have been covered with a thin layer of this paint.

#### 4. Conclusions

The PAMELA magnetic spectrometer has been accurately tested during 2002. The measured spatial resolution is about  $3\mu\text{m}$  in the bending view. Several mechanic and thermal tests have

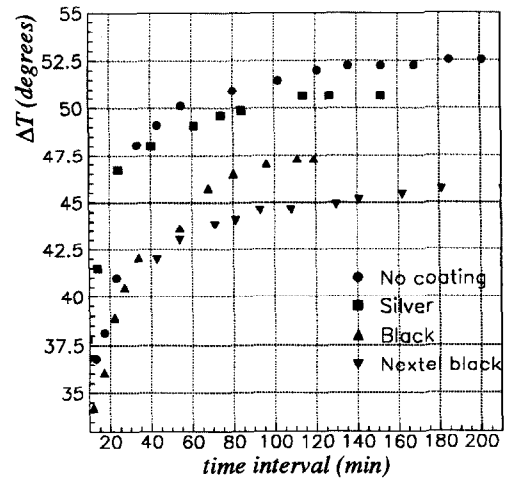


Figure 10. Results of thermal tests done to study the effect of different paints applied on the surfaces of the magnetic cavity (see text for explanations).

been performed to determine the final configuration of the apparatus. The final PAMELA assembly phase is actually in progress and its launch is foreseen at the end of 2003.

#### REFERENCES

1. PAMELA Proposal, July 1996
2. Nucl. Instrum. Methods, **A 478** (2002), 114–118
3. WiZard Collaboration Official WEB Site: <http://wizard.roma2.infn.it/>
4. T. Maeno *et al.*, *Astroparticle Physics*, Vol. 16, Issue 2, November 2001, Pages 121–128
5. M. Aguilar *et al.*, *Physics Reports*, Vol. 366, Issue 6, August 2002, Pages 331–405
6. F. Taccetti *et al.*, *Nuclear Instruments and Methods in Physics Research A* 485 (2002) 78–83
7. O. Adriani *et al.*, *Nuovo Cimento* **112A**, 1317 (1999),
8. Tesi di laurea, Massimo Bongi, Università degli Studi di Firenze, AA 2001–2002